

Interstellar Matter and the Boundary Conditions of the Heliosphere¹

Priscilla C. Frisch

Department of Astronomy and Astrophysics, University of Chicago,
Chicago, Illinois 60637

February 27, 1998

ABSTRACT

The interstellar cloud surrounding the solar system regulates the galactic environment of the Sun, and determines the boundary conditions of the heliosphere. Both the Sun and interstellar clouds move through space, so these boundary conditions change with time. Data and theoretical models now support densities in the cloud surrounding the solar system of $n(\text{H}^\circ)=0.22\pm 0.06\text{ cm}^{-3}$, and $n(e^-)\sim 0.1\text{ cm}^{-3}$, with larger values allowed for $n(\text{H}^\circ)$ by radiative transfer considerations. Ulysses and Extreme Ultraviolet Explorer satellite He° data yield a cloud temperature of 6,400 K. Nearby interstellar gas appears to be structured and inhomogeneous. The interstellar gas in the Local Fluff cloud complex exhibits elemental abundance patterns in which refractory elements are enhanced over the depleted abundances found in cold disk gas. Within a few parsecs of the Sun, inconclusive evidence for factors of 2–5 variation in Mg^+ and Fe^+ gas phase abundances is found, providing evidence for variable grain destruction. In principle, photoionization calculations for the surrounding cloud can be compared with elemental abundances found in the pickup ion and anomalous cosmic ray populations to model cloud properties, including ionization, reference abundances, and radiation field. Observations of the hydrogen pile-up at the nose of the heliosphere are consistent with a barely subsonic motion of the heliosphere with respect to the surrounding interstellar cloud. Uncertainties on the velocity vector of the cloud that surrounds the solar system indicate that it is uncertain as to whether the Sun and $\alpha\text{ Cen}$ are or are not immersed in the same interstellar cloud.

¹Talk at ACE Science Meeting, January 1997, Caltech

1. Introduction

The physical conditions of the surrounding interstellar cloud establish the boundary conditions of the solar system and heliosphere. The abundances and ionization states of elements in the surrounding interstellar cloud determine the properties of the parent population of the anomalous cosmic ray and pickup ion components. In addition, the history of the interstellar environment of the heliosphere appears to be partially recorded by radionucleotides such as ^{10}Be and ^{14}C in geologic ice core records (Sonett et al. 1987, Frisch 1997). Because the solar wind density decreases as R^{-2} (R =distance to Sun), the solar wind and interstellar densities are equal at about 5 AU (the orbit of Jupiter), in the absence of substantial “filtration”². Approximately 98% of the diffuse material in the heliosphere is interstellar gas (Gruntman 1993). Thus, the physical properties of the outer heliosphere are dominated by interstellar matter (ISM). Were the Sun to encounter a high density interstellar cloud, it is anticipated that the physical properties of the inner heliosphere would also be ISM-dominated. Zank and Frisch (1998) have shown that if the space density of the interstellar cloud which surrounds the solar system were increased to $\sim 10\text{ cm}^{-3}$, the properties of the inner heliosphere at the 1 AU position of the Earth would be dramatically altered.

The accuracy with which the physical properties of the surrounding cloud can be derived from observations of stars within a few parsecs of the Sun (1 pc \sim 200,000 AU) depends on the homogeneity and physical parameters of nearby ISM. Observations of nearby stars gives sightlines which probe the ensemble of nearby clouds constituting the “Local Fluff” cloud complex. Conclusions based on observations of nearby stars, however, must be qualified by the absence of detailed data pertaining to the small scale structure of the local ISM (LISM). More distant cold diffuse interstellar gas is highly structured, replete with dense ($\sim 10^4 - 10^5\text{ cm}^{-3}$), small (20–200 AU) inclusions occupying in some cases less than 1% of the cloud volume (Frail et al. 1994, Falgarone et al. 1997, Falgarone and Puget 1995, Heiles 1997). Small scale structures are ubiquitous in interstellar gas, and individual velocity components exhibiting column densities as low as $N(\text{H}^\circ)\sim 3\times 10^{18}\text{ cm}^{-3}$ are found in cold clouds (Frail et al. 1994, Heiles 1997). The presence of dense low column density wisps near the Sun is allowed by currently available data.

The Sun has a peculiar motion with respect to the “Local Standard of Rest” (LSR³);

²“Filtration” refers to the deflection of interstellar H° around the heliopause due to the coupling between interstellar protons and H° resulting from charge exchange

³The LSR is the velocity frame of reference in which the vector motions of a group of nearby comparison stars are minimized. Stars in the LSR corotate around the galactic center with a velocity of $\sim 250\text{ km s}^{-1}$

the Sun moves through the LSR with a velocity $V \sim 16.5 \text{ km s}^{-1}$ towards the apex direction $l=53^\circ$, $b=+25^\circ$ (Mihalas and Binney 1981). Uncertainties on the relative solar-LSR motion appear to be less than 3 km s^{-1} and $\pm 5^\circ$. This motion corresponds to $\sim 17 \text{ pc}$ per million years. Note that the solar path is tilted by $\sim 25^\circ$ with respect to the galactic plane. The Sun oscillates about the galactic plane, crossing the plane every 33 Myrs, reaching a maximum distance from the plane of $\sim 77 \text{ pc}$. The last galactic plane “crossing” was about 21 Myrs ago (Bash 1986). This amplitude of oscillation can be compared to scale heights on the order of $\sim 50\text{-}80 \text{ pc}$ for cold H_2 and CO, $\sim 100 \text{ pc}$ for cold H° and infrared cirrus, $\sim 250 \text{ pc}$ for warm H° , and $\sim 1 \text{ kpc}$ for warm H^+ (the “Reynolds Layer”).

There are three time scales of interest in understanding the environmental history of the solar galactic milieu – $\sim 10^6$ years, $\sim 10^5$ years, and $\sim 10^4$ years. Prior to entering into the Local Fluff complex of interstellar clouds, the Sun traveled through a region of the galaxy between the Orion spiral arm and the spiral arm spur known as the Local Arm. On the order of a million years ago, the Sun was displaced $\sim 17 \text{ pc}$ in the anti-apex direction, which is towards the present day location of the junction of the borders of the constellations of Columba, Lepus and Canis Major. The motions of the Sun and surrounding interstellar cloud with respect to interstellar matter within 500 pc, projected onto the plane, are illustrated in Figure 1. Note that the velocity vectors of the Sun and interstellar cloud surrounding the solar system are nearly perpendicular in the LSR, implying that the surrounding cloud complex is sweeping past the Sun (see section 2). When the morphology of the Local Fluff complex is considered, it is apparent that sometime during the past $\sim 200,000$ years the Sun appears to have emerged from a region of space with virtually no interstellar matter (densities $n(\text{H}^\circ) < 0.0005 \text{ cm}^{-3}$, $n(e^-) < 0.02 \text{ cm}^{-3}$) and entered the Local Fluff complex of clouds (average densities $n(\text{H}^\circ) \sim 0.1 \text{ cm}^{-3}$) outflowing from the Scorpius-Centaurus Association of star-forming regions. One model for the morphology of the cloud surrounding the solar system predicts that sometime within the past 10,000 years, and possibly within the past 2,000 years, the Sun appears to have entered the interstellar cloud in which it is currently situated (Frisch 1994, Frisch 1997). The cloud surrounding the solar system will be called here the “Local Interstellar Cloud” (LIC⁴).

⁴This cloud surrounding the solar system is also referred to as the “surrounding interstellar cloud”, or SIC, which unambiguously defines the cloud feeding interstellar matter into the solar system. For the sake of uniformity of notation, however, the term LIC is used here.

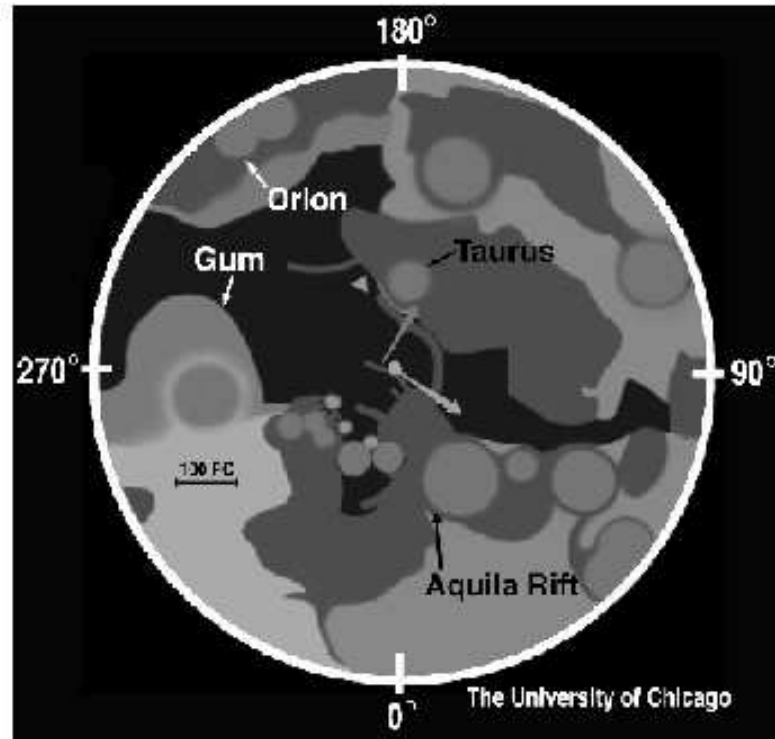


Fig. 1.— The distribution of interstellar molecular clouds (traced by the CO 1- \rightarrow 0 115 GHz rotational transition) and diffuse gas (traced by E(B-V) color excess due to the reddening of starlight by interstellar dust) within 500 pc of the Sun are shown. The round circles are molecular clouds, and the shaded material is diffuse gas. The horizontal bar (lower left) illustrates a distance of 100 pc. Interstellar matter is shown projected onto the galactic plane, and the plot is labeled with galactic longitudes. The distribution of nearby interstellar matter is associated with the local galactic feature known as “Gould’s Belt”, which is tilted by about 15–20° with respect to the galactic plane. ISM towards Orion is over 15° below the plane, while the Scorpius-Centaurus material (longitudes 300°–0°) is about 15–20° above the plane. Also illustrated are the space motions of the Sun and local interstellar gas, which are nearly perpendicular in the LSR velocity frame. The three asterisks are three subgroups of the Scorpius-Centaurus Association. The three-sided star is the Geminga Pulsar. The arc towards Orion represents the Orion’s Cloak supernova remnant shell. The other arcs are illustrative of superbubble shells from star formation in the Scorpius-Centaurus Association subgroups. The smallest (i. e. greatest curvature) shell feature represents the Loop I supernova remnant.

2. Velocity, Magnetic Field

The velocity of the cloud surrounding the solar system provides the sole criteria for selecting LIC absorption features in nearby stars, and therefore for deducing the structure of this cloud.

The velocity of the cloud feeding neutral gas into the solar system is found from backscattered solar He^o 584 A radiation (e. g. Flynn et al. 1998), direct measurements of inflowing He^o atoms by Ulysses (Witte et al. 1993, Witte et al. 1996, Witte, private communication), and measurements of pickup ions (Moebius 1996). In the rest frame of the Sun, the downwind direction of the velocity vector found from He^o backscattered radiation is $V=26.4\pm 1.5$ km s⁻¹, $\lambda=76.0^\circ\pm 0.4^\circ$, $\beta=-5.4^\circ\pm 0.6^\circ$ (ecliptic coordinates), with $T=6,900\pm 600$ K (Flynn et al. 1998). This corresponds to an heliocentric upwind vector in galactic coordinates of $l=4.1^\circ\pm 0.8^\circ$ $b=+14.8^\circ\pm 0.7^\circ$, $V=-26.4\pm 1.5$ km s⁻¹. The Ulysses neutral gas detector yields a downwind vector of $V=25.3\pm 0.5$ km s⁻¹, $\lambda=74.8^\circ\pm 0.5^\circ$, $\beta=-5.7^\circ\pm 0.2^\circ$, $T=6,100\pm 300$ K. The Ulysses vector corresponds to an heliocentric upwind direction in galactic coordinates of $l=3.8^\circ$, $b=+16.0^\circ$.

These determinations of the cloud velocity from measurements of interstellar gas within the solar system can be compared with the values derived from observations of interstellar absorption lines towards the nearest stars. The velocity vector of the surrounding cloud has also been determined by fitting the velocities of interstellar absorption line components in a limited number of nearby stars. The fits by Bertin et al. (1993a) give an upwind direction $V=-25.7$ km s⁻¹, $l=5.9^\circ$, $b=16.7^\circ$, which is consistent with the Ulysses He^o observations. Uncertainties on this velocity are hard to ascertain due to the small number of stars on which the vector derivation is based, but will be assumed to be ± 1.5 km s⁻¹, or $\sim 1/2$ of the typical spectral resolution of the data.

Removing solar motion from these three velocity vectors gives an upwind direction for the LIC cloud in the LSR of $V=-18.7\pm 0.6$ km s⁻¹ from the direction $l=327.3^\circ\pm 1.4^\circ$, $b=0.3^\circ\pm 1.0^\circ$ (Frisch 1995). The Ulysses and EUVE data He^o data indicate a cloud temperature of $T=6,400$ K. As a curiosity, this LSR direction is $\sim 10^\circ$ from the 1.3 pc distant star α Cen. In essence, the Local Fluff gas is sweeping down on the solar system from the vicinity of α Cen.

The small difference in the magnitudes and directions of the Ulysses versus backscatter vectors introduces a significant uncertainty concerning the structure of the Local Fluff and the location of the Sun with respect to the boundary of the surrounding interstellar cloud. The uncertainties on the velocity vectors as defined by the Flynn et al. versus Ulysses versus Bertin et al. (“AG”) vectors do not allow us to make a definitive statement as to

whether or not the Sun and the nearby star α Cen are immersed in the same interstellar cloud. The Flynn et al. vector projected in the direction of the star α Cen ($d=1.3$ pc, $l=315.8^\circ$, $b=-0.7^\circ$) predicts a heliocentric velocity of -16.9 ± 1.0 km s $^{-1}$ for the LIC cloud. The Ulysses flow vector predicts a velocity of -16.2 ± 1.0 km s $^{-1}$. The Bertin et al. AG flow vector predicts a velocity of -15.7 ± 1.0 km s $^{-1}$. The small differences between these three predictions (~ 1.2 km s $^{-1}$) may seem academic, but when compared to observational data these differences have consequences regarding the location of the Sun with respect to the edge of the interstellar cloud in which it is situated. The velocities of the Mg $^+$ and Fe $^+$ absorption lines observed in this direction are -17.5 to -18.2 km s $^{-1}$ with assumed uncertainties on the individual velocities of ± 1.0 km s $^{-1}$ (corresponding to 1/3 of the nominal spectral resolution with which the observations were acquired, Lallement et al. 1995, Linsky and Wood 1997)⁵. As noted by Lallement et al. (Lallement et al. 1995), if the AG velocity vector is correct, less than 2.5×10^{16} cm $^{-2}$ column density of H is found between the Sun and the location of the cloud edge in this direction. This corresponds to a distance to the cloud edge of less than 0.03 pc (6000 AU) for $n(\text{H})=0.3$ cm $^{-2}$ (see section 3). In contrast, if the Flynn et al. vector is correct, the uncertainties allow the Fe $^+$ and Mg $^+$ absorption features to be formed in the surrounding cloud, so that $\log(N(\text{Fe}^+))=12.36$ cm $^{-2}$ towards α Cen (Lallement et al. 1995). Using $\log(N(\text{Fe}^+)/N(\text{H}^+))\sim -5.71$ in the surrounding cloud (Table 1) then indicates that the cloud edge is at or beyond α Cen. Since the star α Cen is located in the true upwind direction (i. e. in the LSR), if the AG vector is correct the Sun would thus exit the cloud now surrounding the solar system within the next 2,000 years, while if the Flynn et al. vector is correct the Sun will not exit the current cloud for over 70,000 years. These data allow, but do not require, the Local Fluff gas to be a structured or turbulent medium on the $\leq 5,000$ AU scale. Evidently reducing these uncertainties in the velocity of the cloud around the solar system will enable us to understand interactions between the Sun and interstellar gas over the next 100,000 years.

The strength of the interstellar magnetic field in the cloud surrounding the solar system has not been directly measured. A strength of ~ 1.6 μG has been found to be consistent with observations of polarization and pulsar dispersion measures (Frisch 1991), while estimates of the heliosphere confinement pressure give an upper limit $B < 3\text{--}4$ μG (Gloeckler et al. 1997). Ultimately, three-dimensional MHD heliosphere models, in comparison with *Voyager* data, may provide the best estimate for the magnetic field strength in the cloud surrounding the solar system. The presence of a local magnetic field is confirmed by observations of the polarization of light from nearby stars ($d < 35$ pc) in the galactic center hemisphere

⁵These data were acquired with the Hubble Space Telescope GHRS instrument at a nominal spectral resolution of 3.3 km s $^{-1}$.

(Tinbergen 1982, Frisch 1991). *If* the cloud surface is perpendicular to the direction of gas flow, then the direction of the magnetic field is found to be approximately parallel to the LIC cloud surface (Frisch 1996). The pile-up of H° at the heliosphere nose is consistent with an interstellar magnetic field strength of $3 \mu\text{G}$ (see section 7).

3. Neutral Density

The quantities of interest in constraining the heliosphere are the absolute neutral and ion space densities (cm^{-3}), which can be derived from column densities (cm^{-2}) only if cloud length is known. The *average* density of nearby gas can be inferred from observations of H° and other elements seen in absorption. For example, combining H° column densities for the six clouds detected towards the four nearby stars α Cen (1.3 pc), α CMa (2.7 pc), α CMi (3.5 pc) and α Aql (5 pc), gives an average density $\langle n(H^\circ) \rangle = 0.08\text{--}0.11 \text{ cm}^{-3}$ for interstellar gas within 3–5 pc of the Sun. This value can be compared with $\langle n(H^\circ) \rangle \sim 0.2 \text{ cm}^{-3}$ for the surrounding cloud, suggesting a filling factor of $\sim 50\%$ ⁶. Data for α Cen and α CMa are given in Table 1. The hydrogen column density for α Aql has been inferred from Ca^+ absorption lines using the conversion factor $N(\text{Ca}^+)/N(\text{H}) \sim 10^{-8}$, based on $N(\text{Ca}^+) \sim 10^{10} \text{ cm}^{-2}$ and $N(H^\circ + H^+) = 10^{18} \text{ cm}^{-2}$ towards η UMa (which samples a low column density sightline through the Local Fluff complex, Frisch and Welty 1998). With this conversion factor, $N(\text{Ca}^+) \sim 1.7 \times 10^{10}$ observed towards α Aql, gives $N(\text{H}) = 1.7 \times 10^{18} \text{ cm}^{-2}$. (The depletion variations of Ca^+ , discussed in section 5, will affect this conclusion.) The average density $\langle n(H^\circ) \rangle \sim 0.10 \text{ cm}^{-3}$ can be used as a guide when inferring the overall morphology of interstellar clouds in the Local Fluff complex.

The absolute space density of the LIC can be inferred from observations of pickup ions combined with the H°/He° ratio in the surrounding cloud (e. g. Gloeckler et al. 1997, Vallerga 1996, Frisch and Slavin 1996). An average value $N(H^\circ)/N(\text{He}^\circ) \sim 14$ is found from observations of white dwarf stars (Dupuis et al. 1995, Frisch 1995, Vallerga 1996, also see section 6). EUVE observations of the two lowest column density white dwarf stars GD 71 ($l=192^\circ$, $b=-5^\circ$, $N(H^\circ) = 8.7 \pm 0.7 \times 10^{17} \text{ cm}^{-2}$) and HZ 43 ($l=54^\circ$, $b=84^\circ$, $N(H^\circ) = 6.3 \pm 1.6 \times 10^{17} \text{ cm}^{-2}$) give $N(H^\circ)/N(\text{He}^\circ)$ ratios of 12.1 and 15.8 respectively over the sightlines to these stars (Vallerga 1996), a difference which may reflect local variations in ionization levels. In principle hydrogen ionization rises towards cloud exterior more rapidly than helium ionization because of the low column densities (Slavin 1989, Cheng and Bruhweiler 1990, Vallerga 1996, Slavin and Frisch 1998a, Slavin and Frisch 1998b), so the actual

⁶The “filling factor” of a cloud complex is the fraction of space occupied by the gas in the complex.

ratio $N(\text{H}^\circ)/N(\text{He}^\circ)$ at the solar location will be larger than the sightline averaged values measured for white dwarf stars. Observations by Ulysses of interstellar helium within the heliosphere yield $n(\text{He}^\circ)\sim 0.016\pm 0.002\text{ cm}^{-3}$ (Witte et al. 1993, Witte et al. 1996, Witte private communication). Combining the Ulysses and EUVE data gives a lower limit on the neutral density in the interstellar cloud outside of the solar system of $n(\text{H}^\circ)=0.22\pm 0.06\text{ cm}^{-3}$, with larger values allowed by the above radiative transfer considerations. Both hydrogen and helium are ionized in the surrounding cloud, however, so the total space density (neutral plus ions) will be larger (see section 5).

Observations of $L\alpha$ backscattered radiation from interstellar hydrogen in the inner heliosphere yield a value $n(\text{H}^\circ)=0.15\pm 0.05\text{ cm}^{-3}$ for the interstellar H° density inside of the heliopause (Quemerais et al. 1995). Combined with the LIC value of $n(\text{H}^\circ)$ above, this gives $\sim 30\%$ filtration of H° at the heliopause.

4. Structure

The largest data set on the Local Fluff complex is derived from observations of the optical Ca^+ H and K lines. Although globally calcium has highly variable depletions onto interstellar dust grains in the ISM, Ca^+ observations constitute the most complete set of available data and therefore provide a first look at the structure and morphology of nearby gas. The rest of this section rests on the assumption that calcium depletions and ionization are relatively constant across the clouds in the Local Fluff cloud complex. This premise may not be true, but it offers an insight into the distribution of ISM within 30 pc of the Sun. Because of the variation of both calcium depletion and ionization in interstellar gas in general, this distance estimate is useful mainly to provide a qualitative picture of the distribution of Local Fluff gas.

About 80 individual Ca^+ velocity components have been observed that can be attributed to the Local Fluff complex (Frisch and Welty 1998). The overall morphology of the Local Fluff complex is shown in Figure 2, where Ca^+ column densities ($N(\text{Ca}^+)$) are plotted versus galactic longitude and latitude for stars sampling the Local Fluff complex. (Data are from Bertin et al. 1993b, Crawford 1994, Crawford and Dunkin 1995, Crawford et al. 1996, Frisch 1997, Lallement et al. 1986, Lallement and Bertin 1992, Lallement et al. 1994, Lallement et al. 1995, Vallerga et al. 1993, Welty et al. 1996, Frisch and Welty 1998.) The well-known asymmetry in the distribution of Local Fluff complex between the galactic center and anti-center hemispheres is apparent. In the absence of data on non-refractory elements in a given sightline, the distance to the “edge” of the Local Fluff cloud complex can be guesstimated using the somewhat uncertain relation for the Local

Fluff $d(\text{pc}) \sim 3 \times 10^{-10} N(\text{Ca}^+)$, for $\langle n \rangle \sim 0.1 \text{ cm}^{-3}$. The sightline to the star τ^3 Eri ($l=214^\circ$, $b=-60^\circ$, $N(\text{Ca}^+)=5 \times 10^{10} \text{ cm}^{-2}$) shows that the Local Fluff complex extends into the southern galactic hemisphere. The low column densities ($N(\text{Ca}^+) < 10^{10} \text{ cm}^{-2}$, Vallerga et al. 1993, Frisch and Welty 1998) towards the three high latitude stars σ Leo ($l=253^\circ$, $b=60^\circ$), η UMa ($l=101^\circ$, $b=65^\circ$), and α^2 CVn ($l=117^\circ$, $b=79^\circ$) show the Sun is “above” most of the mass of the Local Fluff complex (in the sense of “above” the galactic plane). The cloud in front of τ^3 Eri may be an extension of the interstellar cloud complex seen towards α Gru, δ Vel, ϵ Gru, α Hyi, and ι Cen and other nearby stars (with data from Crawford and Dunkin 1995, Lallement et al. 1986, Crawford et al. 1996, Frisch and Welty 1998). The location of the upwind cloud in the LSR (which is the galactic center hemisphere of the sky) coincides with the interstellar dust patch which polarizes the light of nearby stars (Tinbergen 1982, Frisch 1991). This cloud has been identified as part of the leading edge of the 4 Myr old superbubble shell expanding from the last epoch of star-formation in the Scorpius-Centaurus association (Frisch 1995).

The Local Fluff complex is structured and inhomogeneous. At 3 km s^{-1} resolution, about one interstellar absorption line velocity component is seen per 1-2 parsecs of sightline in the direction of the stars α CMa at 2.7 pc and α Aql at 5 pc (Lallement et al. 1994, Lallement et al. 1986), but the actual filling factors of the gas is not known since the densities of LISM clouds other than the LIC are unknown. Globally, cold H° clouds and cold molecular (H_2 , CO) clouds fill $\sim 10^{-3}$ – 10^{-4} of cloud volume, evidently revealing structure consistent with a Kolmogorov spectrum, including features on ≤ 100 AU scale sizes. Ionization also appears to be inhomogeneous, based on both the variations in the white dwarf $N(\text{H}^\circ)/N(\text{He}^\circ)$ ratios and factors of 2–4 variation in LIC electron densities (section 5 and Table 1). Other possible evidence for local structure on subparsec scales are the absence of gas at the LIC velocity in the Fe^+ and Mg^+ lines towards α Cen (1.3 pc) (section 2) and the possible small scale structure (≤ 0.1 pc) revealed by the finite time width of the ^{10}Be spikes in the antarctic ice core record (Frisch 1997). The upper limits on Ca^+ column density towards λ Aql ($l=30^\circ$, $b=-6^\circ$, Vallerga et al. 1993) indicate either the LIC cloud surface is closer than 1.2 pc or that the calcium is doubly ionized in this direction.

5. Ionization

The relative ionizations of elements in interstellar gas at the solar location are a sensitive function of the relative number of EUV (200–900 Å) versus FUV (900–1500 Å) photons, which in turn depends on the mix of different sources of ionizing radiation and radiative transfer in the Local Fluff (e. g. Slavin 1989, Reynolds 1991, Cheng and

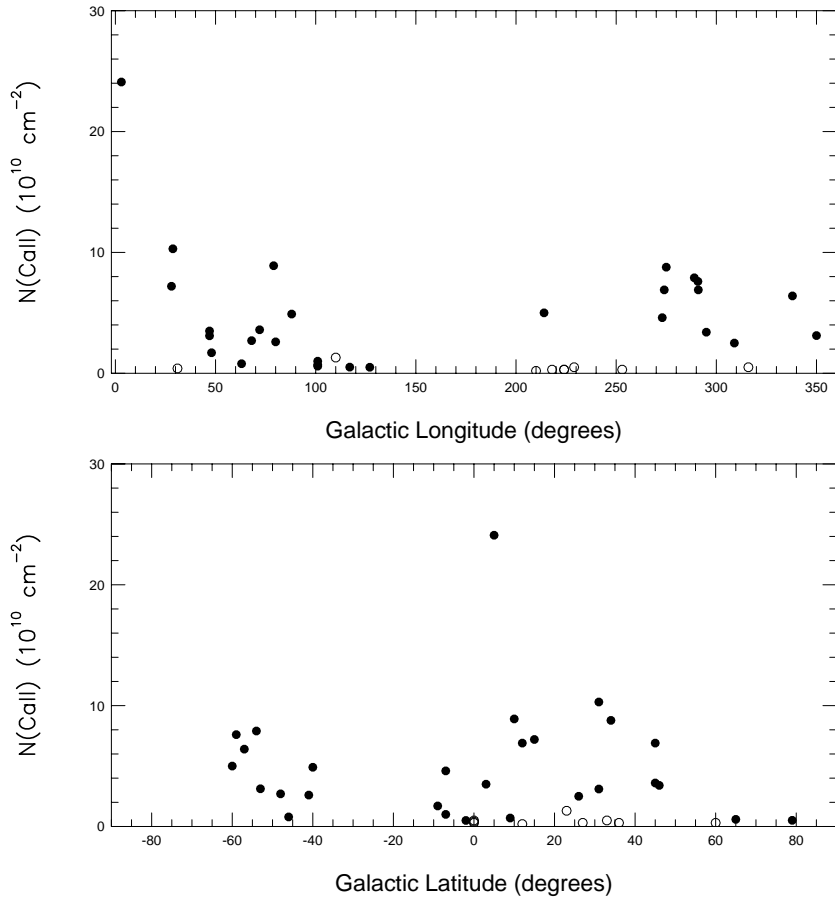


Fig. 2.— Overall morphology of Local Fluff complex of interstellar clouds based on Ca^+ observations of nearby stars. Total Ca^+ column densities for stars sampling the Local Fluff complex are plotted versus galactic longitude and latitude. The open circles are upper limits. With the exception of τ^3 Eri, at $l=214^\circ$, $b=-60^\circ$, $d=17$ pc, the section of the galaxy between $l=130^\circ$ and 270° is relatively devoid of nearby interstellar gas. (Data are from Bertin et al. 1993b, Crawford 1994, Crawford and Dunkin 1995, Crawford et al. 1996, Frisch 1997, Lallement et al. 1986, Lallement and Bertin 1992, Lallement et al. 1994, Lallement et al. 1995, Vallerga et al. 1993, Welty et al. 1996.)

Bruhweiler 1990, Vallerga and Welsh 1995). Locally, hydrogen ionization is dominated by the ultraviolet flux from the star ϵ CMa, a luminous B2 II star located in a direction with very low column densities. The radiation field which ionizes He, Ne, and other species with ionization potentials greater than 13.6 eV is dominated by white dwarf stars, the diffuse soft X-ray flux, and radiation from a predicted conductive interface between the Local Fluff complex and the nominal hot ($\sim 10^6$) plasma filling the adjacent Local Bubble interior (Vallerga 1998, Slavin and Frisch 1998a, Slavin 1989).

The question of which methods to use in calculating interstellar electron densities needs to be put in the context of global ISM studies. Different estimates of interstellar ionization equilibrium towards denser clouds do not produce consistent results. Welty et al. (1998) have observed an $n \sim 10 \text{ cm}^{-3}$ cloud towards the star 23 Ori, and found that thirteen

different ratios of neutral-to-first ionization states yield electron density values that span a range of a factor of 25. Welty attributes this range to a combination of unidentified physical processes (such as charge exchange) and uncertain rate constants. In light of these generic ISM studies, for the LIC a variety of approaches are needed to estimate the electron density.

The electron density in the LIC cloud has been found with several methods, some of which provide cloud-averaged values versus values at the solar location. Based on the results outlined below, it appears that $n(e^-) \sim 0.1 \text{ cm}^{-3}$ in the LIC, but more work is needed. These methods include:

- Observations of absorption lines of trace ions in the LIC cloud as seen towards nearby stars. These data give electron density values that are averaged over the cloud segment being sampled.
- Theoretical predictions of the LIC ionization at the solar location based on a radiation field which is the sum of measurements of ultraviolet and extreme ultraviolet fluxes of point sources such as white dwarf and other hot stars near the Sun. These calculations include radiative transfer effects.
- Theoretical predictions of the LIC ionization, including radiative transfer effects, at the solar location based on a radiation field which is the sum of both a diffuse radiation field (from scattered starlight, plasma in the local hot bubble, and emission from the predicted conductive interface on the LIC cloud) and measurements of ultraviolet and extreme ultraviolet fluxes from point sources such as white dwarf and hot stars near the Sun.
- Measurements of H° , He° , and He^+ in nearby white dwarf stars, which when compared to the nominal reference abundance ratio $N(H^\circ)/N(He^\circ) = 10/1$ gives an estimate of the LIC ionization. This approach gives electron densities averaged over the cloud segment being sampled.
- Theoretical models of the hydrogen wall of the heliosphere, which has properties dominated by charge exchange between interstellar protons and hydrogen atoms piled up at the heliopause. Proton and electron densities are assumed to be equal.

Absorption Line Data: The LIC electron density has been inferred from the ratio Mg^+/Mg° and C^+ fine-structure lines (Frisch et al. 1990, Lallement et al. 1994, Lallement and Ferlet 1996, Gry et al. 1995, Frisch 1994, Lallement 1996, Wood and Linsky 1997). Electron densities found towards nearby stars are $0.09 (+0.23, -0.07) \text{ cm}^{-3}$ towards ϵ CMa (LIC cloud only), $0.11 (+0.12, -0.06)$ towards α Aur, ~ 0.24 towards η UMa, 0.31 ± 0.20

towards δ Cas, and $0.2\text{--}0.4\text{ cm}^{-3}$ towards α CMa (see Table 1). The large value seen towards α CMa may indicate a cloud interface between the LIC cloud ($T\sim 10^4$ K) and adjacent plasma ($T\sim 10^6$ K, Frisch 1994, Bertin et al. 1995). The convergence between the theoretical models (Table 2) and the $n(e^-)$ values from ϵ CMa $\text{Mg}^+/\text{Mg}^\circ$ and α Aur C^+ fine-structure data suggest that the LIC value is $n(e^-)\approx 0.1\text{ cm}^{-3}$. In principle, electron densities can also be inferred from optical observations of Na° and Ca^+ , but as these species are subordinate ionization states of elements with variable depletions in the ISM, and trace ISM at different temperatures, the resulting electron densities are highly uncertain. The range $n(e^-)=0.15\pm 0.11\text{ cm}^{-3}$ is found from Na° data (Lallement and Ferlet 1996, Lallement 1996).

Stellar radiation field: Predicted ionization levels of the LISM depend on whether the radiation field estimates are based on point sources, such as white dwarf and hot stars, or also emission from diffuse hot gas. Including stellar fluxes alone, e. g. ϵ CMa and white dwarf stars, hydrogen is predicted to be $\sim 13\%$ ionized and He $\sim 4.3\%$ ionized at the solar location (Vallerga 1996, Vallerga 1998), yielding $n(e^-)\sim 0.03\text{ cm}^{-3}$

Diffuse and stellar radiation field: Diffuse EUV emission is expected from the Local Bubble 10^6 K plasma and the conductive interface between the LIC and plasma (Slavin 1989). As part of an ongoing project, we (Slavin and Frisch 1998a, 1998b, Frisch and Slavin 1996) are modeling the ionization balance in the LIC using a radiative transfer ionization which includes both diffuse and point source EUV and FUV emission, yielding a self-consistent solution for cloud heating and cooling. The predictions of this model are sensitive to assumptions about the input radiation field and cloud abundances. These results have been calculated using parts per million (PPM) values for He, C, N, O and Ne of 1×10^5 , 191, 85, 646, and 123, respectively, based on LIC abundances towards ϵ CMa (Gry and Dupin 1995). In this particular model hydrogen and helium ionizations are predicted to be $\sim 23\%$ and $\sim 36\%$, respectively, giving $n(e^-)\sim 0.08\text{ cm}^{-3}$ if $n(\text{H})=0.3\text{ cm}^{-2}$. Table 2 shows that these results for He, O, N are consistent with PUI data providing O and N are filtered at the heliopause by $\sim 30\%$. (Alternatively, they could have lower intrinsic abundances.) However, Ne predictions agree with the PUI data only if Ne° increases by a factor of ~ 2.5 . Since Ne is only $\sim 20\%$ neutral at the solar location in this particular model, small changes in the extreme ultraviolet radiation field yield larger changes in the fraction of neutral Ne. Since He has about the same ionization potential, however, this change would create problems in understanding the He data. The model used for the Table 2 predictions yields predictions of $\text{S}^\circ/\text{O}^\circ=2.8 \times 10^{-6}$ and $\text{Mg}^\circ/\text{O}^\circ=2.2 \times 10^{-5}$. These predictions are highly sensitive to the diffuse radiation field in the 200–1200 Å region which has not been directly measured. These results represent one possible model, but better understandings of the radiation field, ISM reference abundances, and cloud geometry are needed before the

problem can be considered solved.

White dwarf stars: The two white dwarf stars with the lowest column densities are GD 71 and HZ 43. EUVE observations of He° and He^+ toward the white dwarf star HZ 43 (a high latitude white dwarf at 60 pc which samples the Local Fluff complex) yield an upper limit on the electron density of $n(e^-) < 0.14 \text{ cm}^{-3}$ for $n(\text{H}^\circ + \text{H}^+) = 0.15\text{--}0.34 \text{ cm}^{-3}$, after comparing $N(\text{H}^\circ)$, $N(\text{He}^\circ)$ and $N(\text{He}^+)$ with the expected cosmic ratio $N(\text{H})/N(\text{He}) = 10/1$ and heliospheric He data (Vallerga 1996).

Hydrogen wall: The observed velocity distribution of interstellar H° decelerated by charge exchange with interstellar protons at the heliopause can be reproduced theoretically in the direction of α Cen for the case where the interstellar gas confining the heliosphere has plasma density $n(e^-) = 0.1 \text{ cm}^{-3}$ (see section 7).

6. Abundances

In principle *in situ* measurements of pickup ions and anomalous cosmic rays can help resolve an active debate as to whether solar or B-star abundances (which are $\sim 70\%$ solar) apply as the correct reference abundance for the interstellar medium.⁷ Since He is primordial, the correct reference ratio H/He ratio should $\sim 10/1$, regardless of whether solar or B-star abundances apply in the ISM. Elements that will be sensitive as to whether the correct ISM reference abundances are solar versus B-star are Ne, Ar, N and S, none of which are thought to be depleted onto interstellar dust grains. Therefore, when LIC ionization and the filtration of elements at the heliopause are properly understood, measurements of N/He, O/He, Ne/He and Ar/He (for example) will constrain the reference abundance of the LIC cloud.

The gas phase abundances of the neutral atomic constituents in the LIC are a function of both the ionization and depletion patterns of the gas. Abundant elements in the ISM such as C, S, Mg, Fe, and Si, have first ionization potentials (FIP) less than the 13.6 eV ionization potential of H° , so they will be predominantly ionized in the LIC. Thus, low-FIP elements will be under-represented in the pickup ion population when compared to cosmic abundances. The relative abundances of common low-FIP elements, based on observations typical of warm and cold gas in interstellar clouds, are shown in Table 3. Absorption lines

⁷The abundances of C, N, O and other elements in the Sun are $\sim 50\%$ higher than abundances in B-stars, and it is an open question as to whether B-star or solar abundances apply to the ISM (Snow and Witt 1996, Savage and Sembach 1996).

from C° , Si° , Fe° , S° are weak in warm low column density ISM.

Table 1: ABUNDANCES IN DIRECTIONS OF NEARBY STARS¹

Star	l, b, r	V_{obs}/V_{LIC} (km s ⁻¹)	Log N(H ^o) (cm ⁻²)	n(H ^o) (cm ⁻³)	n(e ⁻) (cm ⁻³)	Log T (10 ⁴ K)	Log N(Fe ⁺) (cm ⁻²)	Log N(Mg ⁺) (cm ⁻²)	N(O ^o) (cm ⁻²)	$\delta(\text{Fe}^+)/\delta(\text{Mg}^+)/\delta(\text{O}^o)$
α Cen ²	316°, -1°, 1.3 pc	-18/-15.7	17.6-18.0	0.1-0.2		5.4±0.5	12.36±0.07	12.70±0.06		~-0.95/~-0.68/
α CMa ³	227°, -9°, 2.7 pc	19/19.5	17.23±0.17	(0.04) ¹²	0.2-0.4	7.6±3.0	11.93±0.07	12.20±0.08		-0.98/-0.78/
ϵ CMa ⁴	240°, -11°, 187 pc	17/15.6	17.30 ⁸		0.09(+0.23,-0.07)	7.2±2.0	12.13	12.48	14.15	-0.68/-0.40/-0.02
α CMi ⁵	214°, +13°, 3.5 pc	21/19.5	17.88±0.05	0.07		6.9±0.38	12.05±0.02	12.36±0.02		-1.34/-1.10/
α Aur ⁶	163°, +5°, 12 pc	22/22.0	18.24±0.05	0.05	0.11(+0.12,-0.06)	7.0±0.9	12.49±0.03	12.83±0.02		-1.26/-0.99/
δ Cas ⁷	127°, -2°, 27 pc	12.3/12.9			0.30±0.20		12.81±0.09			
G191-B2B ⁹	156°, +8°, 44 pc	20/20.1	18.27	0.01		~7	12.48±0.17	12.72±0.14	14.63	-1.30/-1.13/-0.51
η UMa ¹⁰	101°, +65°, 42 pc	-3.2/-4.8	17.85	0.005	(0.24) ¹¹	(2.7) ¹¹	12.39	12.70	14.27	-0.97/-0.73/-0.45

¹Depletions calculated with respect to H^o only. The depletion of element X is $\text{Log}[X/H]-\text{Log}[X/H]_{solar}$, where solar abundances with respect to hydrogen are: $\text{Log}[O]=-3.13$, $\text{Log}[Fe]=-4.49$, $\text{Log}[Mg]=-4.42$ (Savage and Sembach 1996). For α CMa and ϵ CMa, values are given only for the LIC component.

²Piskunov et al. 1997, Lallement et al. 1995, Crawford 1994, Linsky and Wood 1997

³Lallement et al. 1994, Lallement et al. 1995, Frisch 1994. LIC component only

⁴Gry et al. 1995, Gry and Dupin 1995. LIC component only.

⁵Piskunov et al. 1997, Linsky et al. 1995

⁶Piskunov et al. 1997, Lallement et al. 1995,

⁷Lallement et al. 1995

⁸LIC component only; Vallerga (1996) gives $\text{log}N(\text{H}^o)=17.90$ cm⁻² for the total neutral column density towards this star, based on EUVE data.

⁹Lemoine et al. 1996, Lallement et al. 1995

¹⁰From Frisch 1998, Frisch and Welty 1998, Frisch and York 1991, including preliminary results based on HST GHRS data.

¹¹The electron density is based on the T=2,700 K temperature at which $n(\text{e}^-)$ derived from Mg^o/Mg^+ and C^{+*}/C^+ ratios are equal.

¹²Including the H column density of the second, blue-shifted, cloud gives a total column density of $N(\text{H}^o)=17.53$ cm⁻³ (Bertin et al. 1994).

Table 2: Photoionization Predictions vs. Pick-Up Ion Data*

Ratio	CLOUDY ¹ Predictions	CLOUDY with <i>30% O^o, N^o</i> <i>filtration at heliopause</i>	Pick-Up Ions ²	Anomalous Cosmic Rays ³	Assumed LIC Ratio (no ionization)
He ^o /O ^o	125	178	226±44	13.3	155
N ^o /O ^o	0.12	0.12	0.133 (+0.067,−0.057)	0.15	0.13
Ne ^o /O ^o	0.05	0.08	0.211 (+0.127,−0.086)	0.067	0.19
He ^o /Ne ^o	2330	2330	1031 (+418,−231)	200	813
C ^o /He ^o	1.2 10 ^{−6}		<0.08	1.8 10 ^{−5}	0.0026

* The photoionization code predictions were made with the photoionization code CLOUDY (Ferland 1996). The photoionization code predictions are sensitive to the uncertain diffuse radiation field in the 200 Å – 1200 Å region. The assumed LIC abundances are based on Gry and Dupin (1995) observations towards ϵ CMa.

Refs.

1. These predictions are from Slavin and Frisch (1997a, 1997b) and Frisch and Slavin (1996), using LIC reference abundances (see text).
2. Geiss et al. 1994.; Gloeckler 1996 (private communication)
3. Cummings and Stone (1996).

Table 3: Gas-Phase Neutral Elements in Sample of Interstellar Clouds

Ratio	Log(Ratio)/H ^o	Source	Reference
O ^o /H ^o	−3.19	ϵ CMa LIC	Gry and Dupin (1995)
Mg ^o /H ^o	−4.82	ϵ CMa LIC	Gry and Dupin (1995)
D ^o /H ^o	−5.12	λ Sco warm cloud	York (1983)
N ^o /H ^o	−4.14	λ Sco warm cloud	York (1983)
O ^o /H ^o	−3.37	λ Sco warm cloud	York (1983)
Ar ^o /H ^o	−5.81	λ Sco warm cloud	York (1983)
Na ^o /H ^o	−8.06	ζ Oph warm cloud	Morton (1975)
Mg ^o /H ^o	−8.01	ζ Oph warm cloud	Savage et al. (1992)
C ^o /(H ^o +H ₂)	−5.77	ζ Oph cold cloud	Morton (1975)
Si ^o /(H ^o +H ₂)	≤−8.54	ζ Oph cold cloud	Morton (1975)
Fe ^o /(H ^o +H ₂)	−9.6	ζ Oph cold cloud	Morton (1975)
S ^o /(H ^o +H ₂)	−7.19	ζ Oph cold cloud	Federman and Cardelli (1995)
C ⁺ /H ^o	−3.85	global ISM	Cardelli et al. 1998
N ^o /H ^o	−4.12	global ISM	Meyer et al. 1998a
O ^o /H ^o	−3.50	global ISM	Meyer et al. 1998b

Most elements are not present in solar abundances in interstellar gas, a phenomena explained by invoking the depletion of the missing elements onto dust grains which are mixed into the interstellar gas. Recently arguments have been made that the correct reference abundance for the interstellar medium should be B-star abundances, at about 70% solar (e. g. Snow and Witt 1996), reducing the amount of ISM tied up in grain mass.

Typical gas-to-dust mass ratios of 100:1 are found in the global ISM. Depletion patterns depend on cloud type, and nearby interstellar gas shows enhanced abundances with respect to the abundance patterns seen in distant cold clouds (Frisch 1981). Generally elements with high condensation temperatures (e. g. Si, Mg, Mn, Fe, Cr, Ni, Ca, Co, Ti) are the most depleted in cold clouds. In warm interstellar clouds these refractory elements show less depletion, i. e. have higher gas phase abundances (e. g. see Savage and Sembach 1996). Warm clouds in the galactic halo have similar properties as warm disk clouds (e. g. Fitzpatrick 1996). The abundances of Fe and Mg in Table 1 indicate LISM gas-phase abundance variations of factors of 2–5, suggesting variable grain destruction. In the cold cloud towards the star ζ Oph, 99.4% of Fe and 97% of Mg are depleted onto dust grains. In contrast, ~90% of Fe and ~85% of Mg are depleted onto dust grains in the LIC (Table 1).

These enhanced abundances seen in local gas were the basis for my original conclusion that the interstellar gas surrounding the solar system had been processed through a supernova shock front which had partially destroyed embedded dust grains (Frisch 1981).

Figure 3 shows gas phase abundances of the most common elements, where in this case the solar abundances have been used as the reference abundance for interstellar gas. The gas phase abundances in both warm and cloud clouds are shown. Elements with FIPs less than 13.6 eV will be mainly ionized, whereas O, N, Ar, Ne, He will be primarily neutral when hydrogen is neutral. Also shown are uncertainties in Mg, Fe, Si and O abundances in the LIC. Predicted ratios $\text{Mg}^\circ/\text{O}^\circ=2.2 \times 10^{-5}$ and $\text{S}^\circ/\text{O}^\circ=2.8 \times 10^{-6}$ are deduced from the radiative transfer model with LIC abundances discussed in section 5 and Table 2. Thus, Mg° and S° are candidates for positive detections in the pickup ion population.

Table 1 also summarizes Fe and Mg abundances towards several nearby stars. A puzzling pattern emerges from the data in Table 1. The stars α CMA, ϵ CMA and α Cen, appear to have enhanced $\text{Mg}^+/\text{H}^\circ$ and $\text{Fe}^+/\text{H}^\circ$ abundances in the foreground interstellar gas when compared to the other stars in the table, a property which may be partly attributed to ionization effects which are not included in the depletion estimates. Of the stars listed in Table 1, these three stars sample clouds in the most compact region of space around the solar system. For stars sampling more distant regions, uncertainties could be introduced by unresolved velocity structure in saturated lines, but the good correlation between Fe^+ and Mg^+ suggests this is not the case (Frisch et al. 1998). Alternatively, this variation could be evidence for abundance variations in the gas-phase ISM over the longer sightlines within 20 pc of the Sun (e. g. Lallement et al. 1995, Piskunov et al. 1997, Vallerga and Welsh 1995, Frisch 1995). This variation corresponds to a factor of ~ 4 variation in gas phase abundances, but much smaller variations in dust mass due to the highly depleted nature of refractories.

7. Hydrogen “Wall” at Heliosphere Nose

The relative motions of the Sun and surrounding interstellar cloud result in a pile-up of interstellar H° at the nose of the heliosphere caused by the charge exchange coupling of interstellar H° and H^+ (e. g. Baranov et al. 1971, Baranov and Malama 1993, Gayley et al. 1997, and references therein). This pile-up leaves a signature in the $\text{Ly}\alpha$ absorption line which can, in principle, be distinguished and modeled in the spectrum of nearby stars (Linsky and Wood 1997, Frisch et al. 1996). Gayley et al. (1997) have modeled the $\text{Ly}\alpha$ due to the pile-up in the spectrum of α Cen, and found that a barely subsonic heliosphere model with a Mach number of 0.9 provided the best fit. The model parameters used in this

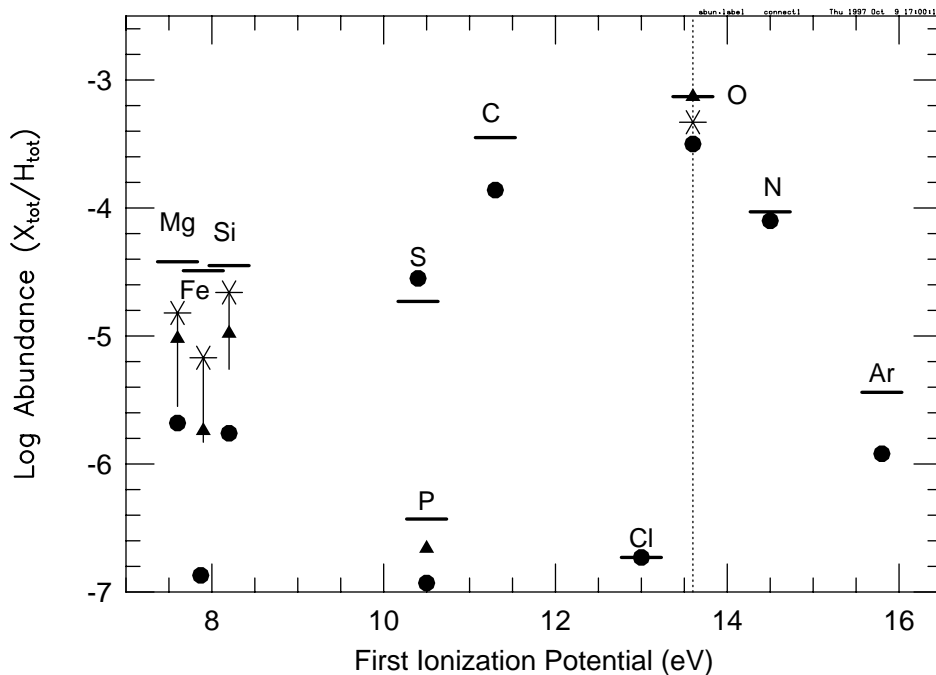


Fig. 3.— The abundances of the most common elements present in interstellar gas are shown plotted against FIP. X_{tot} is the total abundance of element X, while H_{tot} is the total abundance of H. The solar abundances (short line), and typical abundances in warm clouds (triangles) and cold clouds (circle) cloud are shown, based on observations of ζ Oph. (The apparent overabundance of S in cold gas is probably the result of measurement uncertainties.) The vertical bars represent the range of abundances found for the LIC (Table 1); the asterisks are the ϵ CMa LIC values. Since over twelve interstellar absorption components are seen towards ζ Oph, these abundances are guides only to the differences found in abundance patterns. Not shown is the ratio $\text{Na}/\text{H} = -6.64$ in the cold cloud towards ζ Oph, where the ionization potential of Na is 5.1 eV. Elements with FIPs less than 13.6 eV (the hydrogen ionization potential) will be ionized in neutral interstellar clouds. Both abundance patterns and ionization must be considered when estimating the abundances of neutrals in interstellar gas. These abundances, and the reference abundances, are taken from Savage and Sembach (1996), York (1983), and Table 1.

fit were $n(\text{H}^{\circ}) = 0.14 \text{ cm}^{-3}$, $n(e^{-}) = 0.1 \text{ cm}^{-3}$, $T = 7,600 \text{ K}$, and $V = -26 \text{ km s}^{-1}$. For this set of parameters, if the excess velocity (over the sound speed) is the Alfvén speed resulting from an interstellar magnetic field, then a magnetic field strength of $B = 3.1 \mu\text{G}$ is required to achieve a Mach number of 0.9. This gives sound and Alfvén speeds of 10.5 and 20.9 km s^{-1} respectively. Although the full range of parameter space has not yet been explored for the modeling process, supersonic and subsonic models corresponding to Mach numbers 1.5 and 0.7, or magnetic field strengths of 2 and 5 μG , were found to provide unacceptable fits to the observed Ly α profile. Based on this exercise, evidently the properties of astrospheres may be used to determine the pressure of the interstellar medium at the location of a star, as predicted earlier by Frisch (1993).

8. Concluding Remarks

One new conclusion presented here is that in principle the *in situ* pickup ion data can help resolve the outstanding question of whether the correct reference abundances for the LIC are given by solar versus B-star abundances.

A second new result is that the uncertainties on the LIC velocity vector indicate that it is not yet clear whether the Sun and α Cen are immersed in the same interstellar cloud.

Based on the discussions in this paper, the best values for LIC properties are given by $n(\text{H}^\circ)=0.22\pm 0.06 \text{ cm}^{-3}$, $n(e^-)=n(\text{H}^+)=0.1 \text{ cm}^{-3}$, $T=6,900 \text{ K}$ and a relative Sun-cloud velocity of $25.8\pm 0.8 \text{ km s}^{-1}$. However, radiative transfer considerations in the LIC suggest that the quoted neutral density is a lower limit. Ulysses and EUVE observations of He° indicate a cloud temperature of $T=6,400 \text{ K}$. The magnetic field strength is weakly constrained to be in the range of 2–3 μG . Models of the $\text{Ly}\alpha$ absorption line towards α Cen are consistent with an Alfvén velocity of 20.9 km s^{-1} , which in turn is consistent with an interstellar magnetic field of 3 μG in the absence of additional unknown contributions to the interstellar pressure. Ulysses and EUVE observations of interstellar He° within the solar system give an upwind direction for the “wind” of interstellar gas through the solar system, in the rest frame of the Sun, of $V=-25.9\pm 0.6 \text{ km s}^{-1}$ arriving from the galactic direction $l=4.0^\circ\pm 0.2^\circ$, $b=15.4^\circ\pm 0.6^\circ$. Removing solar motion from this vector gives an upwind direction for the LIC cloud in the LSR of $V=-18.7\pm 0.6 \text{ km s}^{-1}$ arriving from the direction $l=327.3^\circ\pm 1.4^\circ$, $b=0.3^\circ\pm 1.0^\circ$.

Through a combination of observations and theory, uncertainties in the LIC electron density are narrowing. Radiative transfer in the sightlines towards nearby stars require that cloud models must be combined with data in order to deduce properties at the cloud location. Radiative transfer models of ionization in the LISM show interesting results, but additional understanding of the input radiation fields is needed. The Local Fluff complex is structured and inhomogeneous. Striking progress would be made in understanding this structure if interstellar absorption lines could be observed at resolutions of $\sim 1 \text{ km s}^{-1}$ in the ultraviolet. The most glaring uncertainty is the absence of detailed knowledge about the interstellar magnetic field. Many of the most abundant elements in the LIC are ionized, and densities of neutral atoms with FIPs less than 13.6 eV are typically down by 1–3 orders of magnitude from the dominant ions. The current approach of trying to understand the interaction of the ISM with the heliopause, from both the outside in and the inside out, is finally bearing fruit.

9. Acknowledgements

I would like to thank John Vallergera and a second “anonymous” referee for thoughtful comments which have improved the quality of this paper. I would also like to thank Dan Welty and Adolf Witt for helpful discussions. I gratefully acknowledge the support of NASA grants NAG5-6188 and NAG5-6405.

REFERENCES

- Baranov, V.B., Krasnobaev, KI., and Kulikovsky, A. 1971, Sov. Phys. Dokl., 15, 791
- Baranov, V.B., and Malama, Y.G., 1993, J. Geophys. Res., 98, 15,157
- Bash, F. 1986, The Galaxy and the Solar System, eds. R. Smoluchowski, J. N. Bahcall, M. Matthews, Univ. of Arizona Press, Tucson, AZ, 83
- Bertin, P., Lallement, R., Ferlet, R., and Vidal-Madjar, A., 1993a, J. Geophys. Res., 98, 15193
- Bertin, P., Lallement, R., Ferlet, R., and Vidal-Madjar, A., 1993b, A&A, 278, 549
- Bertin, P., Vidal-Madjar, A., Lallement, R., Ferlet, R., Lemoine, M. 1994, A&A, 302, 889
- Cardelli, J. A., Meyer, D. M., Jura, M., and Savage, B. D. 1996, ApJ, 467, 344
- Cheng, K.-P. and Bruhweiler, F. C. 1990, ApJ, 364, 573
- Cummings, A. C., and Stone, E. C. 1996, Space Sci. Rev., 78, 117
- Crawford, I., A. 1994, The Observatory, 114, 288
- Crawford, I. A., and Dunkin, S. K. 1995, MNRAS, 273, 219
- Crawford, I. A., Craig, N., and Welsh, B. Y. 1997, A&A, 317, 889
- Dupuis, J., Vennes, S., Pradhan, A. K., and Thejll, P. 1995, ApJ, 455, 574
- Falgarone, E. 1997, IAU Colloquium No. 166, Garching, Germany
- Falgarone, E., and Puget, J.-L. 1995, A&A, 293, 840
- Ferland, G. J. 1996, *Hazy, a Brief Introduction to Cloudy*, University of Kentucky Department of Physics and Astronomy Internal Report
- Fitzpatrick, E. L. 1996, ApJ, 473, L55
- Flynn, B., Vallergera, J., Dalaudier, F., Gladstone, G. R. 1998, J. Geophys. Res., in press
- Federman, S. R., and Cardelli, J. A. 1995, ApJ, 452, 269
- Frail, D. A., Weisberg, J. M., Cordes, J. M., Mathers, C. 1994, ApJ, 436, 144

- Frisch, P., Dorschner, J., Geiss, J., Greenberg, M., Gruen, E., Landgraf, M., Hoppe, P., Jones, A., Kraetschmer, W., Linde, T., Morfill, G., Reach, W., Slavin, J., Svestka, J., Witt, A., and Zank, G. 1998, in preparation
- Frisch, P. C. 1981, *Nature*, 293, 377
- Frisch, P. C., and York, D. G. 1991, in *Extreme Ultraviolet Astronomy*, pp. 322–332, Pergamon Press, Eds. R. F. Malina and S. Bowyer
- Frisch, P. C., Welty, D. E., York, D. G., and Fowler, J. 1990, *ApJ*, 357, 514
- Frisch, P. C. 1991, p. 19 in *Physics of the Outer Heliosphere*, COSPAR Colloquia Series, Vol. 1., Eds. S. Grzedzielski and D. E. Page.
- Frisch, P. C. 1993, *ApJ*, 407, 198
- Frisch, P. C. 1997, submitted to *Science*
- Frisch, P. C. 1994, *Science*, 265, 1423
- Frisch, P. C. 1995, *Space Sci. Rev.*, 72, 499
- Frisch, P. C. 1996, *Space Sci. Rev.*, 78, 213
- Frisch, P. C., Welty, D. E., Pauls, H. L., Williams, L. L., and Zank, G. P. 1996, *BAAS*, 28, 760
- Frisch, P. C. and Welty, D. G., 1998, in preparation
- Frisch, P. C., and Slavin, J. D. 1996, *Space Sci. Rev.*, 78, 223
- Gayley, K. G., Zank, G. P., Pauls, H. L., Frisch, P. C. and Welty, D. E. 1997, *ApJ*, 487, 259
- Geiss, J., Gloeckler, G., Mall, U., von Steiger, R., Galvin, A. B., and Ogilvie, K. W. 1994, *A&A*, 282, 924
- Gloeckler, G., Fisk, L. A., and Geiss, J. 1997, *Nature*, 386, 374.
- Gruntman, M. A. 1993, *Planet. Space Sci.* 41, 307
- Gry, C., Lemonon, L., Vidal-Madjar, A., Lemoine, M., and Ferlet, R. 1995, *A&A*, 302, 497
- Gry, C., and Dupin, O. 1995, *Science with the Hubble Space Telescope – II*, P. Benvenuti, u F. D. Macchetto, and E. J. Schreier, Paris, France

- Heiles, C. 1997, *ApJ*, 481, 193
- Lallement, R., Vidal-Madjar, A., and Ferlet, R. 1986, *A&A*, 168, 225
- Lallement, R., and Bertin, P. 1992, *A&A*, 266, 479
- Lallement, R., Bertin, P., Ferlet, R., Vidal-Madjar, A., Bertaux, J. L. 1994, *A&A*, 286, 898
- Lallement, R., Bertin, P., Ferlet, R., Vidal-Madjar, A., Bertaux, J. L. 1995, *A&A*, 304, 461
- Lallement, R., and Ferlet, R. 1996, *A&A*, in press
- Lallement, R., 1996, *Space Sci. Rev.*, 78, 361
- Lemoine, M., Vidal-Madjar, A., Ferlet, R., Bertin, P., Gry, C., and Lallement, R. 1996, *A&A*, 308, 601
- Linsky, J. L., and Wood, B. E., 1997, *ApJ*, 463, 254
- Meyer, D. M., Cardelli, J. A., and Sofia, U. J. 1998a, *ApJ*, in press
- Meyer, D. M., Jura, M. and Cardelli, J. A. 1998b, *ApJ*, in press
- Mihalas, D., and Binney, J. 1981, *Galactic Astronomy Structure and Kinematics*, W. H. Freeman & Co.: San Francisco
- Moebius, E. 1996, *Space Sci. Rev.*, 78, 375
- Piskunov, N., Wood, B. E., Linsky, J. L., Dempsey, R. C., and Ayres, T. R. 1997, *ApJ*, 474, 315
- Quemerais, E., Bertaux, J. L., Sandel, B. R., and Lallement, R., 1996, *A&A*, 308, 279
- Reynolds, R. J. 1991, p. 101 in *Physics of the Outer Heliosphere*, COSPAR Colloquia Series, Vol. 1., Eds. S. Grzedzielski and D. E. Page.
- Savage, B. D., and Sembach, K. R. *ARA&A*, 34, 279
- Slavin, J. D. 1989, *ApJ*, 346, 718
- Slavin, J. D., and Frisch, P. C. 1998a, “Local Bubble and Beyond - IAU Colloquium No. 166”, *Lecture Notes in Physics*, Eds. Breitschwerdt and Freyberg (Springer-Verlag)
- Slavin, J. D., and Frisch, P. C. 1998b, in preparation
- Snow, T. P., Witt, A. N. 1996, *ApJ*, 468 , L65

- Sonett, C. P., Morfill, G. E., and Jokipii, J. R. 1987, *Nature*, 330, 458
- Tinbergen, J. 1982, *A&A*105, 53
- Vallerga, J. 1996, *Space Sci. Rev.*, 78, 277
- Vallerga, J. 1998, *ApJ*, volume 487
- Vallerga, J. V., and Welsh, B. Y. 1995, *ApJ*, 444,702
- Vallerga, J. V., Vedder, P. W., Craig, N., and Welsh, B. Y. 1993, *ApJ*, 411, 729
- Welty, D. E., Hobbs, L. M., Lauroesch, J., Morton, D. C., Spitzer, L., York, D. G. 1998, in preparation
- Welty, D. E., Morton, D. C., Hobbs, L. M. 1996, *ApJS*, 106, 533
- Witte, M., Rosenbauer, H., Banaskiewicz, M., and Fahr, H. 1993, *Adv. Sp. Res.*, 13, 121
- Witte, M., Banaskiewicz, M., Rosenbauer, H., 1996, *Adv. Sp. Res.*, 78, 289
- Wood, B. E., Linsky, J. L. 1997, *ApJ*, 474, 39
- York, D. G. 1983, *ApJ*, 264, 172
- Zank, G., and Frisch, P. C. in preparation